

Structural characteristics of $\text{GdCo}_{1-x}\text{Cr}_x\text{O}_3$ ($x = 0, 0.33, 0.5, 0.67, 1$) perovskites

S. Dimitrovska-Lazova^{1*}, D. Kovacheva², P. Tzvetkov²

¹ University “St. Cyril and Methodius”, Faculty of Natural Sciences and Mathematics, Arhimedova 5, Skopje, R. Macedonia

² Institute of General and Inorganic Chemistry, Bulgarian Academy of Science, “Acad. Georgi Bonchev” bl. 11, 1113 Sofia, Bulgaria

Received March 21, 2012; Revised May 2, 2012

In this paper the synthesis, crystal structure determination and calculation of structural parameters within the $\text{GdCo}_{1-x}\text{Cr}_x\text{O}_3$ ($x = 0, 0.33, 0.5, 0.67$ and 1) are presented. The compounds were synthesized by solution combustion method starting with the nitrates of the constituent metals and urea as a fuel. The perovskites within the series crystallize in *Pnma* with $Z=4$. The lattice parameters and distances and angles were used to calculate several crystallographic parameters such as, cell distortion, orthorhombic distortion, bond and angle deformation, the tilting angles, bond valences, and global instability index. These were used to obtain a clearer picture of the influence of substitution of Co^{3+} with Cr^{3+} in these complex perovskites on the distortion and stability of the perovskite structure.

Key words: complex perovskites, X-ray diffraction, crystal structure, crystallographic parameters.

INTRODUCTION

The role of the perovskites in science and technology is constantly increasing. This is a result of numerous possibilities for application of these materials due to their interesting physical and chemical properties. For example these compounds exhibit wide spread of conducting properties from insulators to conductors, superconductivity, colossal magnetoresistance, giant magneto resistance, catalytic activity toward different catalytic reactions, etc [1–3]. These properties are connected to specific structural characteristics of perovskites as well as with characteristic properties of constituting elements.

Perovskites are usually designated with the formula ABX_3 , where A and B are cations and X is the anion. The positions of the cations may be occupied by different metals from the periodic table, while as an anion most frequently oxygen can be found but there are compounds with halogenides, OH^- , CN^- , or H^- anion. The diversity in perovskite structure is a result of possible multiple substitutions in the

positions of the cations, leading to a great number of so-called complex perovskites.

The ideal perovskite structure is fairly simple. Namely, in cubic unit cell B-cations are surrounded by six anions arranged in octahedral geometry sharing the same vertex. This arrangement forms cubooctahedral cavity in which the A-cation is placed. This structure is very flexible. Namely, the BO_6 octahedra may be rotated to small angle leading to structural distortions and lowering of the cubic symmetry. As a result, large number of distorted (orthorhombic, tetragonal, hexagonal etc.) perovskites are known.

In the present study the structural investigation of complex perovskites with cobalt and chromium ($3+$) cations in B-position is presented. Our focus is on structural changes driven by mutual substitution of these ions in $\text{GdCo}_{1-x}\text{Cr}_x\text{O}_3$ ($x = 0, 0.33, 0.5, 0.67$ and 1) solid solution. The role of cobalt ion in perovskites on their properties is thoroughly studied [4–8] and it is evident that this cation is responsible for a number of interesting properties found in cobalt-containing perovskites. Thus, as a result of possible temperature driven spin state change of Co^{3+} and of its oxidation state, Co-containing perovskites exhibit interesting electrical and magnetic properties, as well as, pronounced catalytic activity [3, 9]. The change in oxidation state of Co^{3+} ion (to Co^{2+} or

* To whom all correspondence should be sent:
E-mail: sandra@pmf.ukim.mk

Co^{4+} state) is accompanied with appearance of vacancies or change of oxidation state of other cations in the compound, while the spin state directly influences the deformation of the structure as a result of the fact that from the three possible spin states of the cobalt ion (low, intermediate and high spin state) the intermediate and high spin state of Co^{3+} exhibit Jahn-Teller effect.

On the other hand, rare earth chromites are interesting because of their electrical conductivity, resistance to oxidation and high melting points [10].

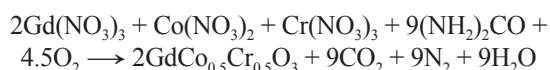
The literature data for the end members of the series $GdCo_{1-x}Cr_xO_3$ ($x = 0, 0.33, 0.5, 0.67$ and 1), $GdCoO_3$ and $GdCrO_3$, showed that these compounds may be synthesized using different methods such as: solid state reaction [11, 12–16], sol-gel method [17–19], synthesis using complex precursors [20–22], hydrothermal method [23, 24], self-propagating high-temperature synthesis [10], decomposition or combustion synthesis using citric acid [9, 25] and by decomposition of nitrate salts [7, 26]. In this study, the solution combustion method was used for the synthesis of investigated compounds. Namely, in recent years the combustion synthesis is becoming one of the most popular methods for obtaining wide variety of oxide materials. Combustion synthesis is fast and inexpensive that enables producing homogeneous, very fine, crystalline, multicomponent oxide powders, without intermediate decomposition steps [27, 28]. It involves highly exothermic reaction between oxidant (usually nitrate salts of metal ions) and an organic fuel. The aim to use this fuel is to be a source of C and H, which are reducing elements in the combustion reaction. The most often used compounds as fuels are: urea, glycine, sucrose, alanine, citric acid, etc. The pathway of the reaction and the temperature of the synthesis are highly dependent on the ratio between fuel and oxidizer (metal nitrates) [29]. This ratio is usually set to 1, but it may be smaller (to 0.7) or bigger than 1. In this study nitrates of the consisting metals were used as oxidizers and the fuel was urea. The ratio between them was set to 1.

The formation of the perovskite phase was examined by X-ray diffraction. The crystallographic characteristics of the end members of the series, $GdCoO_3$ and $GdCrO_3$, are known from the literature [10, 13, 14, 16, 17, 23, 24]. These compounds are orthorhombic and they belong to $GdFeO_3$ -type perovskites (space group $Pnma$). To the best of our knowledge, the intermediate members of the solid solution are synthesized for the first time and we expected that they have the same crystallographic characteristics as the end members. The refinement of the crystal structure confirmed that Co^{3+} and Cr^{3+} ions are completely interchangeable and may be substituted in the whole region of x (from 0 to 1).

EXPERIMENTAL

The starting materials for the synthesis were nitrates of the consisting metals: $Gd(NO_3)_3 \cdot 6H_2O$, $Co(NO_3)_2 \cdot 6H_2O$ and/or $Cr(NO_3)_3 \cdot 9H_2O$. The nitrates were dissolved in small amount of deionised water. The obtained solutions were thoroughly mixed together. As previously mentioned the fuel (F) to oxidizer (O) ratio was set to 1 and according to the stoichiometry, the quantity of the fuel was calculated separately for each compound. The calculated amount of urea was dissolved in 1:1 solution of nitric acid and was added to the solution of metal ions. The final solution was transferred to muffle furnace and heated up to ~ 500 °C. After the evaporation of the water the combustion reaction started and was followed by large emission of gasses CO_2 , N_2 and H_2O . The resulting products were substances, which showed voids, pores, and were highly friable. All powders were black except $GdCrO_3$ that has pale green color.

The combustion reaction for one of the systems may be presented as follows:



The obtained powders were hand grinded and subjected to additional heating at 800 °C for 4h.

The resulting powders were analyzed by X-ray diffraction. The XRD patterns were recorded on *Bruker D8 Advance* with $Cu_{K\alpha}$ radiation and SolX detector within the range 10–120° 2 θ at room temperature with step scanning rate of 0.02°. The crystal structures were refined by the method of Rietveld (program Fullprof).

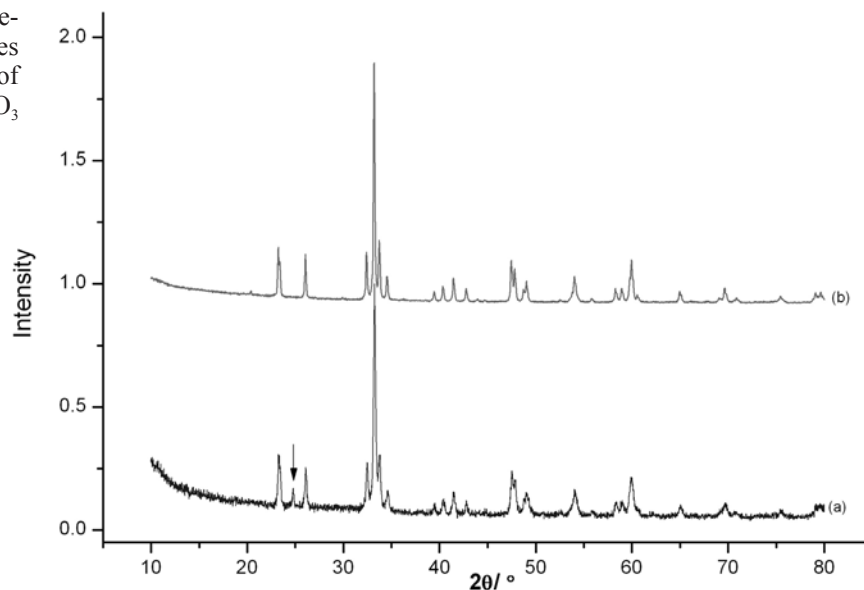
RESULTS AND DISCUSION

The XRD analysis of the powders obtained after the combustion reaction showed that perovskite phase was formed only in the case of $GdCrO_3$, right after the combustion of the initial solution. This as-prepared phase contains small quantity of impurity identified as $GdCrO_4$. The impurities were removed by additional heating of the obtained $GdCrO_3$ perovskite at 800 °C (Fig. 1).

In the case of the other samples the perovskite phase was not formed directly after the combustion reaction, but by further heating at 800 °C for 4 hours. The perovskite structure of the resulting powders was confirmed according to the XRD patterns (Fig. 2).

The analysis of the XRD patterns of the synthesized compounds showed continuous shift of the positions of the diffraction peaks towards lower values with increasing x (Fig. 2). As expected, this shift

Fig. 1. XRD patterns of a) as-prepared GdCrO_3 (the arrow indicates the peak suggesting presence of GdCrO_4 as impurity) and b) GdCrO_3 heated for 2h at 800°C



is a result of the continuous substitution of smaller Co^{3+} ion ($r(\text{Co}^{3+}) = 0.545 \text{ \AA}$) with the larger Cr^{3+} one ($r(\text{Cr}^{3+}) = 0.65 \text{ \AA}$), leading to increasing of the lattice parameters from GdCoO_3 to GdCrO_3 . These results showed that these two ions may be substituted in the whole range of x (from $x = 0$ to $x = 1$) and continuous solid solution may be formed.

The crystal structures of the perovskites within the $\text{GdCo}_{1-x}\text{Cr}_x\text{O}_3$ ($x = 0, 0.33, 0.5, 0.67$ and 1) series were refined using the Rietveld method (program Fullprof) and starting with the structural model of

GdCrO_3 [30]. All perovskites within this series crystallize in $Pnma$ space group ($Z = 4$) (Table 1). The selected distances and angles are given in Table 2.

The structural data for GdCoO_3 and GdCrO_3 are already reported in the literature, and the crystallographic data for mixed Co^{3+} , Cr^{3+} perovskites are given in this paper. The refined values of the unit cell parameters for GdCoO_3 , $a = 5.39074(12)$, $b = 7.45514(17)$ and $c = 5.22527(12)$ are close to the literature values [14, 16] and the obtained values for GdCrO_3 , $a = 5.52447(12)$, $b = 7.60552(16)$ and

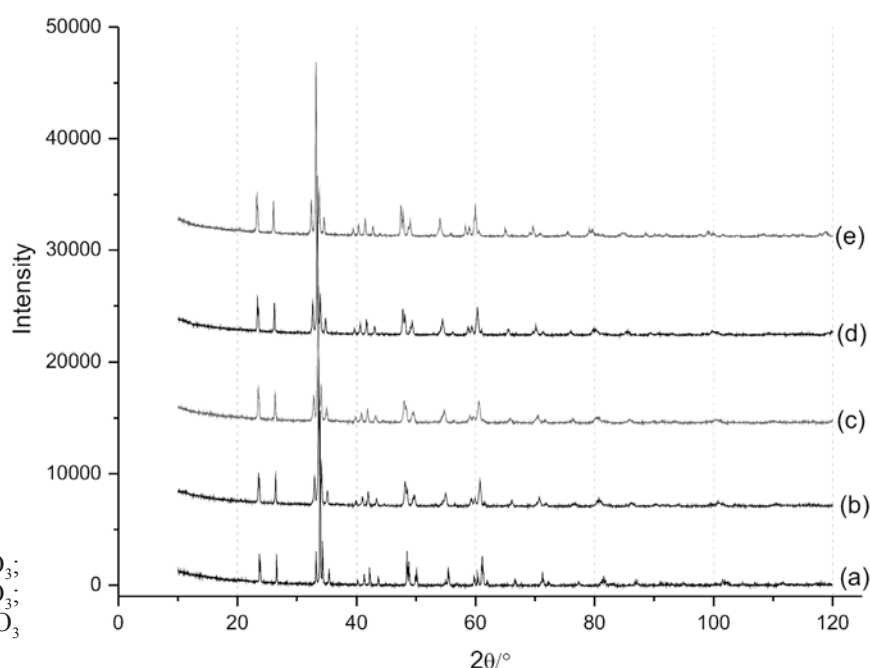


Fig. 2. XRD patterns of a) GdCoO_3 ; b) $\text{GdCo}_{0.67}\text{Cr}_{0.33}\text{O}_3$ c) $\text{GdCo}_{0.5}\text{Cr}_{0.5}\text{O}_3$; d) $\text{GdCo}_{0.33}\text{Cr}_{0.67}\text{O}_3$ and e) GdCrO_3 heated 4h at 800°C

Table 1. Structural data from X-ray powder diffraction studies of $\text{GdCo}_{1-x}\text{Cr}_x\text{O}_3$ perovskites

Atoms	Parameters	GdCoO_3	$\text{GdCo}_{0.67}\text{Cr}_{0.33}\text{O}_3$	$\text{GdCo}_{0.5}\text{Cr}_{0.5}\text{O}_3$	$\text{GdCo}_{0.33}\text{Cr}_{0.67}\text{O}_3$	GdCrO_3
	a (Å)	5.39074(12)	5.4357(3)	5.4573(3)	5.4832(2)	5.52447(12)
	b (Å)	7.45514(17)	7.5046(4)	7.5280(4)	7.5572(3)	7.60552(16)
	c (Å)	5.22527(12)	5.2541(3)	5.2685(3)	5.28499(20)	5.31310(11)
Gd	x	0.05792(19)	0.05740(18)	0.05808(16)	0.05827(14)	0.05890(12)
	z	0.9870(5)	0.9858(4)	0.9850(3)	0.9860(3)	0.9852(2)
	B	0.06(4)	0.07(4)	0.17(3)	0.08(3)	0.25(2)
Co/Cr	B	0.08(7)	0.19(6)	0.12(5)	0.19(5)	0.01(4)
O1	x	0.4816(17)	0.4750(16)	0.4734(14)	0.4744(14)	0.4701(12)
	z	0.085(2)	0.0861(19)	0.0855(17)	0.0940(15)	0.0942(13)
	B	1.5(3)	1.8(3)	1.7(3)	1.4(3)	1.8(2)
O2	x	0.2958(17)	0.2949(15)	0.2969(14)	0.2960(12)	0.2968(10)
	y	0.0461(11)	0.0496(10)	0.0483(10)	0.0479(8)	0.0497(7)
	z	0.7085(18)	0.7091(17)	0.7056(15)	0.7022(13)	0.7035(10)
	B	0.5(3)	0.3(3)	0.5(2)	0.42(19)	0.87(16)
R_i	R_p	22.9	17.6	16.6	15.4	12.1
	R_{wp}	13.9	13.2	12.9	12.2	10.6
	R_{exp}	12.57	10.92	11.16	10.87	9.82
	χ^2	1.22	1.45	1.35	1.25	1.16
	R_B	5.78	4.43	3.17	3.07	2.45

$c = 5.31310(11)$, are also in good agreement to the literature values [13, 23].

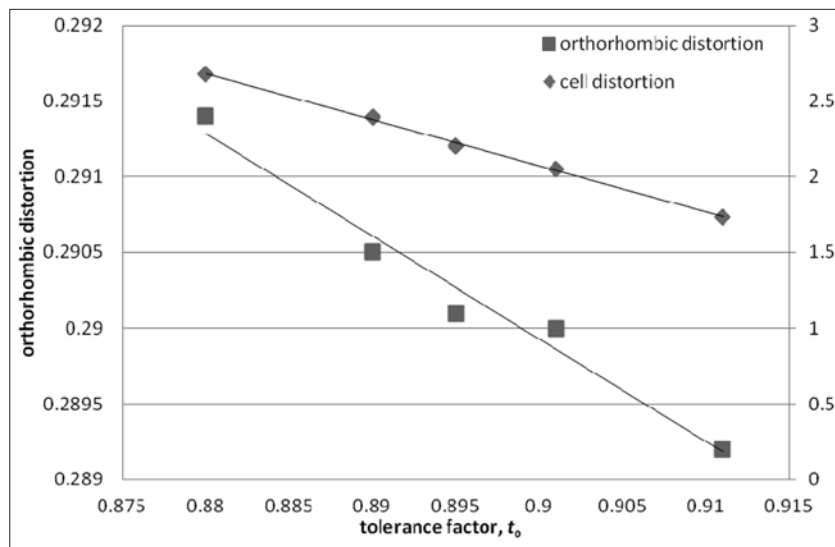
In a series of solid solutions like this one it is important to investigate the structural distortions and the stability of the compounds resulting from the substitution of one cation with another. So, below is given the thorough structural study of the perovskites within this series. In order to quantify the structural distortion of the perovskite structure, usually the first step is to calculate the well known Goldschmidt tolerance factor, t [31]. It is calculated according to

the equation $t = (r(A) + r(O))/\sqrt{2}(r(B) + r(O))$, taking into account the ionic radii of the constituent metals regarding the A-cation as twelve coordinated, and B-cation and O as six coordinated. The boundaries of t for perovskite structure are from 0.78–1.05 [32], and it is expected that in compounds with increasing distortion from ideal perovskite structure the tolerance factor will shift to lower values. The obtained t -values for the investigated compounds are at the lower limit for perovskite structure and are suggesting distorted structures. The values of

Table 2. Selected distances and angles in $\text{GdCo}_{1-x}\text{Cr}_x\text{O}_3$ perovskites

	GdCoO_3	$\text{GdCo}_{0.67}\text{Cr}_{0.33}\text{O}_3$	$\text{GdCo}_{0.5}\text{Cr}_{0.5}\text{O}_3$	$\text{GdCo}_{0.33}\text{Cr}_{0.67}\text{O}_3$	GdCrO_3
Gd – O1	3.149	3.209	3.234	3.252	3.304
Gd – O1	2.341	2.33	2.328	2.352	2.344
Gd – O1	3.017	3.038	3.041	3.1	3.117
Gd – O1	2.274	2.293	2.31	2.267	2.288
Gd – O2 x 2	2.464	2.458	2.484	2.506	2.508
Gd – O2 x 2	2.313	2.312	2.312	2.322	2.329
Gd – O2 x 2	3.323	3.36	3.384	3.4	3.434
Gd – O2 x 2	2.614	2.66	2.65	2.648	2.679
$\langle \text{Gd} - \text{O} \rangle_9$	2.490	2.502	2.508	2.519	2.531
Co – O1 x 2	1.919	1.935	1.941	1.959	1.9731
Co – O2 x 2	1.962	1.979	1.983	1.977	2
Co – O2 x 2	1.91	1.928	1.941	1.965	1.971
$\langle \text{Co} - \text{O} \rangle_6$	1.930	1.947	1.955	1.967	1.981
B – O1 – B	152.56	151.74	151.77	149.43	149.01
B – O2 – B	151.6	150.7	150.3	150.1	149.6

Fig. 3. Relationship between the tolerance factor and the orthorhombic distortion and distortion of the unit cell in the analyzed series $GdCo_{1-x}Cr_xO_3$



t for the investigated series are decreasing from 0.911 for $GdCoO_3$ to 0.880 for $GdCrO_3$ (Table 3).

Both end members of the series $GdCoO_3$ and $GdCrO_3$ are orthorhombically distorted perovskites [13, 14, 16, 23]. As expected, the middle members of the series are also distorted orthorhombic perovskites and the values of the unit cell parameters are increasing from $GdCo_{0.67}Cr_{0.33}O_3$ to $GdCrO_3$ (Table 1). The relationship between the unit cell parameters in

these compounds is $b > c/\sqrt{2} > a$ as in O-type perovskites, where the tilting of the octahedra is the primary source of deformation (Fig. 3). This trend is maintained throughout the entire series. Using the values of the unit cell parameters two crystallographic parameters were calculated – cell distortion [33] and orthorhombic distortion [6] (Table 3). The obtained values point out that the distortion of the unit cell (from ideal cubic) increases with Cr con-

Table 3. Crystallographic parameters of $GdCo_{1-x}Cr_xO_3$ perovskites

	$GdCoO_3$	$GdCo_{0.67}Cr_{0.33}O_3$	$GdCo_{0.5}Cr_{0.5}O_3$	$GdCo_{0.33}Cr_{0.67}O_3$	$GdCrO_3$
t	0.911	0.901	0.895	0.89	0.88
cell distortion	1.731	2.048	2.199	2.395	2.677
orthorhom. distortion	0.2892	0.2900	0.2901	0.2905	0.2914
Δ_9	7.906	8.634	8.374	9.459	9.779
Δ_{10}	12.727	14.138	14.244	15.234	16.186
Δ_6	0.138	0.134	0.103	0.014	0.044
$\theta/^\circ$	13.722	14.131	14.116	15.283	15.493
$\varphi/^\circ$	9.931	9.763	10.362	10.62	10.571
$\Phi/^\circ$	16.882	17.119	17.448	18.538	18.683
BV-A	3.276	3.219	3.16	3.12	3.04
BV-Co	2.721	2.598	2.544	2.46	/
BV-Cr	/	3.287	3.218	3.112	2.995
GII	0.199	0.189	0.183	0.161	0.054

Note: For the calculation of cell distortion first the value of a_p (pseudocubic a parameter) was found according the equation: $ap = (a/\sqrt{2} + b/\sqrt{2} + c/2)/3$ and then it was used to obtain the cell distortion as: $[(a/\sqrt{2} - a_p)^2 + (b/\sqrt{2} - a_p)^2 + (c/2 - a_p)^2]/3a_p$ [33]. The orthorhombic distortion was calculated using the equation: $\{[\Sigma(a_i - a)^2]^{1/2}\}/a$, where $a_i = a, b, c/\sqrt{2}$ and a is an average of a_i [6]. The calculation of the polyhedron bond length distortion parameters Δ_9, Δ_{10} and Δ_6 was performed using the equation: $\Delta = \Sigma[(r_i - r)/r]/n \times 10^3$, where r_i is individual bond length (A - O or B - O), r is the average bond length and n is a number of bonds [34]. The tilt angles are calculated using the fractional atomic coordinates of oxygen atoms [1]. For the calculation of bond valence the used equations are: $s_i = \exp(r_o - r_{ij})/B$ and $BV = \Sigma s_i$, where r_o is empirical parameter, r_{ij} is the bond distance and $B = 0.37$ [35]. The global instability index was calculated using the equation $GII = [(\Sigma d_i^2)/N]^{1/2}$, where d_i is the discrepancy between calculated BV and theoretical oxidation number [36].

tent. These results are in accordance with expected increase in the deformation of the structure obtained from the values of the tolerance factor.

The refined values of the fractional atomic coordinates (Table 1) were used to calculate different structural parameters. These parameters were also used to analyze the contribution of the particular cation in the compound to the structural distortions within the series. Firstly, the change in the surrounding of the gadolinium ion was considered. In the ideal cubic perovskites the coordination of the A-cation is 12 but in orthorhombic perovskites the coordination number is usually lowered to 10, 9 or 8. In this series of perovskites the coordination of Gd^{3+} is becoming more distorted as the content of Cr^{3+} is increasing. This may be noticed from the values of the Gd–O distances, which are increasing with enhancement of the substitution of Co^{3+} ion. As a consequence, the coordination number of Gd^{3+} changes and it is lowered from 10 in GdCoO_3 to 9 in GdCrO_3 . This effect is also obvious from the values of the polyhedron bond length distortion Δ_9 and Δ_{10} . Namely, these parameters are reflecting the deformation of the distances in the coordination polyhedron. It may be noticed that the highest values are obtained for GdCrO_3 .

Contrary to the trend in deformation of the coordination of gadolinium ion the deformation of the B-cations (Co^{3+} and/or Cr^{3+}) octahedra is decreasing from GdCoO_3 to GdCrO_3 (Table 3). Although the Co/Cr–O bond lengths (Table 2) are increasing the polyhedron bond length distortion parameter, Δ_6 , is decreasing (Table 3) in the same direction. This parameter shows that the distortion of the bonds in the octahedra is decreasing and the octahedron is becoming more regular. The obtained values for the first members of the series are relatively high, especially if we compare them to the values of Δ_6 in ferrites (GdFeO_3 , $\Delta_6 = 0.032$) [1], but they remain still smaller than the values found in manganites, where

Mn^{3+} is a Jahn-Teller ion (GdMnO_3 , $\Delta_6 = 6.701$) [37]. It is interesting to note that as the octahedron becomes more regular across the series, the tilt angles are increasing. Namely, if the values of the tilt angles (φ , θ , and Φ), calculated using the atomic coordinates of oxygen atoms [1] are compared, it could be stated that these values are increasing with increasing of x . From these results it may be concluded that importation of chromium ion in place of Co^{3+} makes the octahedron more regular in respect to its bond lengths but in the same time it is more tilted.

The increase in the tilting angle of the octahedra is reflected in lowering of the B–O1–B and B–O2–B angles. From Table 2 it is evident that these angles are substantially different from 180° – the value characteristic for ideal cubic perovskites. These low values are suggesting smaller Co/Cr-3d and oxygen-2p orbital overlap. Namely, as the angle is increased and approaches 180° , a greater overlap is achieved. This overlap directly controls the interaction integral β , which is proportional to the width of the Co/Cr–O bands [38].

The bond length and the valence of the bond are related in the bond valence model given by I. D. Brown [35]. The calculated values of the bond valence of cations are also presented in Table 3. It is obvious that there are positive and negative deviations from the theoretical values of the oxidation states of the cations. The values for the Gd^{3+} and Cr^{3+} ions are larger than the theoretical ones, which suggests that the average Gd–O and Cr–O distances in these compounds are shorter than the average bond distances in other oxides containing Gd or Cr compounds. It is also obvious that the values for the bond valence of cobalt ion are becoming smaller throughout the series (Table 3) with pronounced differences from the theoretical value. The values for the bond valence are used to calculate the global instability index,

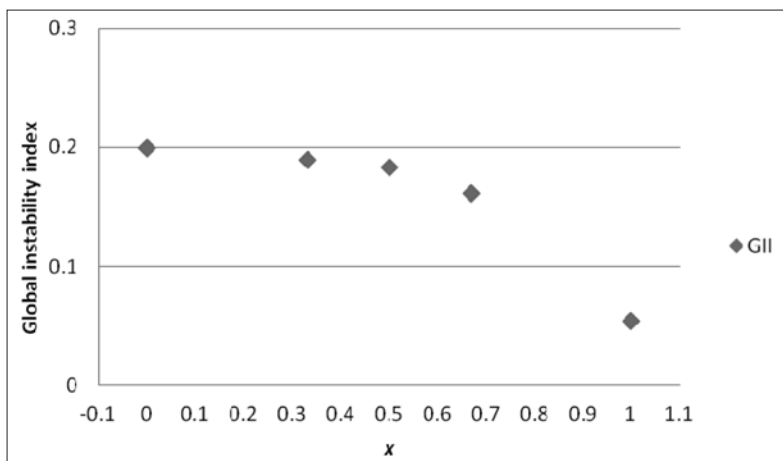


Fig. 4. Change of the global instability index with increasing x in the series $\text{GdCo}_{1-x}\text{Cr}_x\text{O}_3$

GII. This index reflects the overall stress in the structure. The values of GII are usually smaller than 0.1 in structures without internal stress, the values between 0.1 and 0.2 are characteristic for compounds with lattice-induced strains, and higher than 0.2 - for unstable structures [36]. From the calculated values of GII it may be pointed that $GdCrO_3$ (GII = 0.054) meets the requirement for structure without internal stress (Fig. 4) and GII for cobalt containing compounds within the series (of values between 0.1 and 0.2) indicate existence of lattice-induced strains.

CONCLUSION

The complex perovskites of general formula $GdCo_{1-x}Cr_xO_3$ ($x = 0, 0.33, 0.5, 0.67$ and 1) were obtained by solution combustion method using urea as a fuel. The Rietveld refinement of the crystal structures showed that they crystallize in *Pnma* with $Z = 4$. According to the lattice parameters and the distances and angles in the compounds, several important parameters were calculated indicating the influence of the mutual substitution of Co^{3+} with Cr^{3+} to the distortion and stability of the perovskite structure. Thus, it was concluded that by increasing of the content of Cr^{3+} ions in the perovskite structure the BO_6 octahedron becomes more regular but the tilting of octahedron is more pronounced. Also the deformation of Gd-O polyhedron increases with increasing of the Cr^{3+} content. The calculated bond valences and global instability indices indicate for existence of lattice-induced strains in the structure of the cobalt containing compounds.

Acknowledgements: The authors thank the National Science Fund of Bulgaria and the Ministry of Education and Science of Republic of Macedonia for the financial support under contract DNTS/Macedonia 01/7/08.12.2011.

REFERENCES

1. R. H. Mitchell, *Perovskites: Modern and Ancient*, Almaz press – Thunder Bay, 2002.
2. F. S. Galasso, *Perovskites and High Tc Superconductors*, Gordon and Breach Science Publishers, 1990.
3. M. A. Peña, J. L. G. Fierro, *Chem. Rev.*, **101**, 1981 (2001).
4. T. Ishihara (Ed), *Perovskite Oxide for Solid Oxide Fuel Cells (Fuel Cells and Hydrogen Energy)*, Springer, Dordrecht, 2009.
5. S. Yamaguchi, Y. Okimoto, Y. Tokura, *Phys. Rev. B*, **54**, R11022 (1996).
6. K. Knížek, Z. Jirák, J. Hejtmánek, M. Veverka, M. Maryško, G. Maris, T. T. M. Palstra, *Eur. Phys. J. B*, **47**, 213 (2005).
7. A. Fondado, J. Mira, J. Rivas, C. Rey, M. P. Breijo, and M. A. Señaris-Rodríguez, *J. App. Phys.*, **87**(9), 5612 (2000).
8. H. W. Brinks, H. Fjellvåg, A. Kjekshus, B. C. Hauback, *J. Solid State Chem.*, **147**, 464 (1999).
9. J.-W. Moon, Y. Masuda, W.-S. Seo, K. Koumoto, *Mater. Sci. Eng. B*, **85**, 70 (2001).
10. M. V. Kuznetsov, I. P. Parkin, *Polyhedron*, **17**, 4443 (1998).
11. A. K. Tripathi, H. B. Lal, *J. Mater. Sci.*, **17**, 1595 (1982).
12. B. Rajeswaran, D. I. Khomskii, A. Sundaresan, C. N. R. Rao, *Phys. Rew. B*, in press.
13. K. Yoshii, *J. Solid State Chem.*, **159**, 204 (2001).
14. S. V. Kurgan, G. S. Petrov, L. A. Bashkirov, A. I. Klyndyuk, *Inorg. Mater.*, **40**, 1224 (2004).
15. H. B. Lal, R. D. Dwivedi, K. Gaur, *J. Mater. Sci.: Mater. Electron.*, **1**, 204 (1990).
16. W. Wei-Ran, X. Da-Peng, S. Wen-Hui, D. Zhan-Hui, X. Yan-Feng, S. Geng-Xin, *Chin. Phys. Lett.*, **22**, 2400 (2005).
17. P. S. Devi, *J. Mater. Chem.*, **3**, 373 (1993).
18. R. A. da Silva, R. N. Saxena, A. W. Carbonari, G. A. Cabrera-Pasca, *Hyperfine Interact.*, **197**, 53 (2010).
19. N. B. Ivanova, N. V. Kazak, C. R. Michel, A. D. Balaev, S. G. Ovchinnikov, A. D. Vasil'ev, N. V. Bulina, E. B. Panchenko, *Phys. Solid State*, **49**, 1498 (2007).
20. P. A. Brayshaw, A. K. Hall, W. T. A. Harrison, J. M. Harrowfield, D. Pearce, T. M. Shand, B. W. Skelton, C. R. Whitaker, A. H. White, *Eur. J. Inorg. Chem.*, 1127 (2005).
21. Y. Seto, K. Umemoto, T. Aarii, Y. Masuda, *J. Therm. Anal. Calorim.*, **76**, 165 (2004).
22. R. Sawano, Y. Masuda, *J. Therm. Anal. Calorim.*, **92**, 413 (2008).
23. K. Sardar, M. R. Lees, R. J. Kashtiban, J. Sloan, R. I. Walton, *Chem. Mater.*, **23**, 48 (2011).
24. A. Jaiswal, R. Das, S. Adyanthaya, P. Poddar, *J. Nanopart. Res.*, **13**, 1019 (2011).
25. A. Patil, S. C. Parida, S. Dash, V. Venugopal, *Thermochimica Acta*, **465**, 25 (2007).
26. F. H. M. Cavalcante, A. W. Carbonari, R. F. L. Malavasi, G. A. Cabrera-Pasca, R. N. Saxena, J. Mestnik-Filho, *J. Magn. Magn. Mater.*, 320, 32 (2008).
27. A. L. A. da Silva, G. G. G. Castro, M. M. V. M. Souza, *J. Therm. Anal. Calorim.*, 1000 (2011).
28. K. C. Patil, M. S. Hegde, T. Rattan, S. T. Aruna, *Chemistry of nanocrystalline oxide*, World Scientific Publishing, Singapore, 2008.
29. A. S. Mukasyan, C. Costello, K. P. Sherlock, D. Lafarga, A. Varma, *Sep. Purif. Technol.*, **25**, 117 (2001).
30. JCPDS International Center for Diffraction Data, Power Diffraction File (entry 00-025-1056), Swarthmore, PA, 1995.
31. V. M. Goldschmidt, *Naturwiss.*, **14**, 477485 (1926).
32. P. M. Woodward, *Acta Cryst.*, **B53**, 44 (1997).
33. G. Huo, D. Song, Q. Yang, F. Dong, *Ceram. Int.*, **34**, 497 (2008).
34. R. D. Shannon, *Acta Crystallogr.*, **A32**, 751 (1976).

35. I. D. Brown, D. Altermatt, *Acta Crystallogr.*, **B41**, 244 (1985).
36. M. W. Lufaso, P. M. Woodward, *Acta Crystallogr.*, **B57**, 725 (2001).
37. Y. Chen, H. Yuan, G. Li, G. Tian, S. Feng, *J. Cryst. Growth*, **305**, 242 (2007).
38. G. Ch. Kostogloudis, N. Vasilakos, Ch. Ftikos, *Solid State Ionics*, **106**, 207 (1998).

СТРУКТУРНО ХАРАКТЕРИЗИРАНЕ НА $GdCo_{1-x}Cr_xO_3$ ($x = 0, 0.33, 0.5, 0.67, 1$) ПЕРОВСКИТИ

С. Димитровска-Лазова^{1*}, Д. Ковачева², П. Цветков²

¹ Университет „Св. Кирил и Методии“, Факултет по Естествени науки и Математика,
Архимедова 2, Скопие, Македония

² Институт по обща и неорганична химия, Българска академия на науките,
„Акад. Г. Бончев“ бл.11, София, България

Постъпила на 21 март, 2012 г.; приета на 2 май, 2012 г.

(Резюме)

В статията са представени синтез, определяне на кристалната структура и калкулирани структурни параметри за серията $GdCo_{1-x}Cr_xO_3$ ($x = 0, 0.33, 0.5, 0.67$ и 1). Съединенията са получени по метода на комбустия през разтвор, като са използвани нитрати на съответните метали и урея за гориво. Серията получени перовскити кристализират в пространствена група $Rnma$, $Z = 4$. Определените параметри на елементарната клетка, разстояния и ъгли са използвани за пресмятане на някои кристалографски параметри, като дисторзия на елементарната клетка, орторомбична дисторзия, деформация на разстояния и ъгли, ъгли на накланяне, сума на валентните връзки и глобален индекс на нестабилност. Тези параметри са използвани да се изясни по-добре влиянието на заместването на Co^{3+} с Cr^{3+} върху степента на деформация и стабилност на перовскитовата структура.